Molecular Cancer Therapeutics

Photodynamic Therapy Using Photosensitizer-Encapsulated Polymeric Nanoparticle to Overcome ATP-Binding Cassette Transporter Subfamily G2 Function in Pancreatic Cancer

Yoon Jin Roh[1], Ju Hee Kim[1], In-Wook Kim[1], Kun Na[2], Jae Myung Park[1,3], and Myung-Gyu Choi[1,3]

Abstract

Chlorin-based photosensitizers are commonly used in photodynamic therapy (PDT). These drugs are effluxed by cell membrane transporters, such as the ATP-binding cassette subfamily G member 2 (ABCG2). PDT efficacy is limited in tumor cells expressing high levels of these proteins. Pancreatic cancer cell lines AsPC-1 and MIA PaCa-2, which have high and low ABCG2 expression, respectively, were used, and ABCG2-overexpressing MIA PaCa-2 cells were generated. We compared PDT efficacy between chlorin e6 (Ce6) and cationic photosensitizer–encapsulated polymeric nanoparticle (PS-pNP), which is comprised with Ce6, polyethylene glycol, and polyethylenimine. The intracellular concentration of Ce6 was significantly higher in MIA PaCa-2 cells than in AsPC-1 or ABCG2-overexpressing MIA PaCa-2 cells. PS-pNP increased intracellular levels of the photosensitizer in all cell lines. The cell viability experiments indicated increased Ce6 resistance in ABCG2-overexpressing cells. In contrast, PS-pNP produced similar levels of cytotoxicity in each of the cancer cell lines tested. Singlet oxygen production was higher in cells treated with PS-pNP than in those treated with Ce6. Furthermore, in heterotopic and orthotopic AsPC-1 xenograft mouse models, PDT using PS-pNP significantly reduced tumor volume in comparison with that of Ce6 treatment. PS-pNP could increase intracellular Ce6 concentration, which was related with reduced ABCG2-mediated efflux of Ce6, thereby enhancing the effects of PDT in pancreatic cancer cells. *Mol Cancer Ther; 16(8); 1487–96. ©2017 AACR.*

Introduction

The prognosis of patients with pancreatic cancer is very poor (1). Curative surgical removal is the best therapeutic option; however, more than 80% of patients are not candidates for surgery and have been treated with chemotherapy or radiotherapy (2). Nevertheless, these treatments offer poor clinical outcomes, as most patients are diagnosed at an already advanced stage of disease and because pancreatic tumor cells exhibit low chemo- or radiosensitivity. Thus, novel therapeutic modalities are needed for treatment of pancreatic cancer.

Photodynamic therapy (PDT) has been clinically applied to the treatment of malignant, cardiovascular, dermatologic, and ophthalmic diseases (3). PDT involves the usage of chemical photosensitizers that are preferentially taken up and retained by diseased cells. Photoactivation of these photosensitizers, by exposure to light of the appropriate wavelength, results in the production of cytotoxic materials, such as singlet oxygen ($^1O_2$), which then cause irreversible damage to the target cells (3). Compared with current cancer treatments, including surgery, radiotherapy, and chemotherapy, PDT offers the advantage of a selective method of destroying diseased tissues without damaging the healthy surrounding areas. An additional advantage is that the photosensitizers used in PDT emit fluorescence upon irradiation, making them useful for both therapy and diagnosis, that is, theranosis (4). PDT eradicates pancreatic carcinoma, both *in vivo* and *in vitro*, without affecting the adjacent normal tissues (5–7). In addition, in a phase I clinical study, administration of PDT resulted in tumor cell necrosis in a group of 16 patients diagnosed with inoperable pancreatic adenocarcinoma (8).

ATP-binding cassette subfamily G member 2 (ABCG2) is a member of the ABC transporter family of proteins and is primarily located within the plasma membrane (9, 10). ABCG2 protein was initially described in doxorubicin-resistant breast cancer cells and has been shown to pump photosensitizers out of the transporter-expressing cells, including chlorin-based photosensitizers, and to thereby inhibit PDT-induced cytotoxicity in target cells (11–13). Interestingly, ABCG2 is overexpressed in pancreatic cancer tissues and in the side population cells of pancreatic cell lines (14, 15).

Our group developed a nanophotosensitizer using the polyelectrolyte complexes between a photosensitizer-encapsulated polymeric nanoparticle (PS-pNP). This compound is composed of polyethylene glycol (PEG), polyethylenimine (PEI), and chlorin e6 (Ce6) and exhibits increased solubility and stability

[1]Catholic Research Institute of Medical Science, The Catholic University of Korea, Seoul, Korea. [2]Department of Biotechnology, Center for Photomedicine, The Catholic University of Korea, Bucheon-si, Gyeonggi-do, Korea. [3]Division of Gastroenterology, Department of Internal Medicine, College of Medicine, The Catholic University of Korea, Seoul, Korea.

Note: Supplementary data for this article are available at Molecular Cancer Therapeutics Online (http://mct.aacrjournals.org/).

Corresponding Authors: Jae Myung Park, The Catholic University of Korea, 222 Banpo-daero, Seocho-gu, Seoul 06591, Republic of Korea (South). Phone: 822-2258-6023; Fax: 822-2258-2055; E-mail: parkjerry@catholic.ac.kr; and Myung-Gyu Choi, Phone: 822-2258-6017; Fax: 822-2258-2055; E-mail: choim@catholic.ac.kr

doi: 10.1158/1535-7163.MCT-16-0642

compared with unmodified Ce6 in the aqueous-phase Chlorin (16). In this study, we demonstrate that PDT-induced cytotoxicity was significantly higher in low ABCG2-expressing pancreatic cancer cells than in high ABCG2-expressing cells. Furthermore, we show that the limited efficacy of chlorin-based PDT in cells expressing high levels of ABCG2 can be enhanced using PS-pNP.

Materials and Methods

Materials

Ce6 was purchased from Frontier Scientific, Inc. Branched PEI (bPEI), with a molecular weight (mol. wt.) of 1,800 Da, was purchased from Alfa Aesar. 1,3-Dicyclohexylcarbodiimide (DCC), N-(3-dimethylaminopropyl)-N′-ethylcarbodiimide hydrochloride (EDC), N-hydroxysuccinimide (NHS), 4-dimethylaminopyridine (DMAP), methoxypolyethylene glycol (mPEG), with a molecular weight of 5,000 Da, 3-(4,5-dimethyl-2-thiazolyl)-2,5-diphenyl-2H-tetrazolium bromide (MTT), esterase from the porcine liver, hyaluronidase from sheep testes (type II), and anhydrous DMSO were purchased from Sigma Aldrich Co.. The dialysis membrane was obtained from Spectrum Laboratories Inc. DMEM, FBS, antibiotics (penicillin/streptomycin), and Dulbecco's PBS were obtained from Gibco BRL (Invitrogen Corp.). All chemicals and solvents were of analytic grade, and mPEG-NHS (5 kDa) was prepared following a published protocol (17).

Synthesis of cationic PS-pNP

The mPEG (5 kDa)-bPEI (1.8 kDa) was synthesized via the conventional carbodiimide reaction. The mPEG-NHS (5 kDa, 3 g) was dissolved in chloroform (30 mL) at room temperature, and then bPEI (0.36 g) was added. The coupling reaction was allowed to occur for 72 hours at room temperature. The reaction mixture was then poured into diethyl ether to precipitate the product. Unreacted mPEG homopolymer and bPEI were eliminated by dialyzing against water using a dialysis membrane (Spectra/Por; mol. wt. cut-off size, 12,000) against deionized water for 2 days. The final products were lyophilized. ^{1}H NMR spectra was recorded in deuterated chloroform (CDCl3) solvent at room temperature using a Bruker NMR Spectrometer (Bruker). To synthesize PS-pNP, Ce6 was also attached to the amine groups of mPEG-bPEI via the conventional carbodiimide reaction. The mPEG-bPEI (1 g) and a mixture of Ce6 (e.g., 0.07 mmol), DCC (1.2 × Ce6 in moles), and N-hydroxysuccinimide (HOSu; 1.2 × Ce6 in moles) were dissolved separately in DMSO (20 mL), and the solutions were stirred thoroughly for 3 hours prior to the condensation reaction. Two reactant solutions were mixed and stirred at room temperature. After 24 hours, the reaction solution was filtered to remove insoluble byproducts (e.g., dicyclohexylurea) and the filtrate dialyzed using a dialysis membrane (Spectra/Por; mol. wt. cut-off size, 1,000) against deionized water for 2 days. The final products (Ce6 conjugates) were lyophilized. mPEG-bPEI-Ce6 synthesis was verified by ^{1}H NMR, and ^{1}H NMR spectra was recorded in DMSO at room temperature using a Bruker NMR Spectrometer. Ce6 contents of the Ce6 conjugates were measured by ultraviolet visible (UV-Vis) spectroscopy (663 nm).

Cells

The human pancreatic cancer cell lines AsPC-1 and MIA PaCa-2 were obtained from Korean Cell Line Bank, which were passaged for fewer than 6 months after resuscitation. For preparation of ABCG2-overexpressing pancreatic cancer cells, retrovirus encoding *ABCG2* genes was produced by using *BglII/XhoI* sites. HEK293T cells were transfected with pMSCV-*ABCG2*, pGag-pol, and pVSV-G, using Lipofectamine 2000, and then 48 hours later, media including Prx III retroviruses were collected and filtered to remove cell debris. MIA PaCa-2 cells were incubated with ABCG2 retrovirus, and the cells were inoculated with ABCG2 retrovirus. The cells expressing ABCG2 were selected with puromycin.

RNA isolation and quantitative RT-PCR

Cells (AsPC-1, MIA PaCa-2, MIA PaCa-2/ABCG2) used for qRT-PCR experiments were washed once with PBS, and RNA was extracted using TRIzol reagent (Invitrogen), per the manufacturer's instructions. cDNA was generated by reverse transcription, using 3 μg of purified RNA and the PrimeScript RT Reagent Kit (TaKaRa), per the manufacturer's instructions. Real-time PCR was performed using a LightCycler 2.0 system (Roche) with SYBR Premix Ex Taq (TaKaRa), according to manufacturer's instructions. The primers used for PCR amplification were BCRP1/ABCG2: 5′- TCA TCA GCC TCG ATA TTC CAT CT-3′ and 5′- GGC CCG TGG AAC ATA AGT CTT-3′. The amplification conditions were 95°C for 30 seconds, 60°C for 30 seconds, and 72°C for 30 seconds, for 40 cycles.

Western blotting

Protein extracts from all cell lines (AsPC-1, MIA PaCa-2, MIA PaCa-2/ABCG2) were prepared in 30 μg quantities. Proteins were separated by 10% SDS-PAGE, transferred to nitrocellulose membranes, and incubated with ABCG2 (SC-377176; Santa Cruz Biotechnology, Inc) and β-actin–specific primary antibodies (SC-47778; Santa Cruz Biotechnology, Inc.). Membranes were then washed and incubated with horseradish peroxidase–labeled secondary antibodies diluted in Tris-buffered saline containing 0.1% Tween 20 and 5% skim milk. Immune complexes were visualized using enhanced chemiluminescence detection reagents, and images were recorded on a LAS-3000 (FUJIFILM) after various lengths of exposure.

Fluorescence microscopy

A total of 1×10^5 cells per well (AsPC-1, MIA PaCa-2, or MIA PaCa-2/ABCG2) were seeded in 6-well plates and incubated overnight at 37°C in a humidified 5% CO_2 atmosphere. The medium was then replaced with 2 mL of fresh medium containing 5 μmol/L Ce6 or PS-pNP. After 6 hours of incubation, cells were washed twice with PBS (1 mL), and fresh medium was added (1 mL). Fluorescence was measured by excitation of Texas Red using a Zeiss fluorescence microscope (Axiovert 200 MAT, Zeiss).

Fluorometer analysis of intracellular photosensitizer levels

A total of 1×10^5 cells per well (2-mL cell suspension of AsPC-1, MIA PaCa-2, or MIA PaCa-2/ABCG2) were seeded in 6-well plates. The medium was then replaced with 2 mL of fresh medium containing 5 μmol/L of Ce6 or PS-pNP and incubated for 6 to 48 hours under the previously described conditions. The solutions were removed, and the cells were rinsed with PBS (1 mL). Then, the cells were harvested by treatment with 300 μL trypsin [0.25%)/ethylene diamine tetraacetic acid (Corning CellGro)]. The trypsin was quenched by addition of fresh medium (0.5 mL), and the solution was transferred to centrifuge tubes (1.5 mL) and centrifuged at 10,000 rpm for 5 minutes. Pellets were then washed with PBS (1 mL) and centrifuged again. The fluorescence of the supernatants was measured using a Synergy

MX fluorometer (BioTek) with excitation and emission wavelengths of 500 and 670 nm, respectively. A calibration curve was then used to calculate the concentrations of Ce6 and PS-pNP per 10,000 cells.

Cell viability

AsPC-1, MIA PaCa-2, and MIA PaCa-2/ABCG2 cells were cultured in RPMI1640 (Corning CellGro) or DMEM (Corning CellGro) supplemented with 10% FBS and 1% penicillin–streptomycin (Penicillin G, sodium salt; streptomycin sulfate) at 37°C in a humidified 5% CO_2 atmosphere. The cells were seeded in 96-well plates at a density of 1×10^4 cells per well (in triplicate) in complete medium, incubated overnight at 37°C; the cells were incubated for 6 hours with indicated concentration of Ce6 or PS-pNP in the presence or absence of 1 μmol/L Ko-143. The cells were then photoirradiated using a diode laser emitting red light at 670 nm wavelength (equipment by Kuk-Je A& SL Co.). The power density at the illumination area was 800 mW/cm^2 (11 minutes 25 seconds) and total light dose was 6 J/cm^2. After irradiation, the cells were incubated for 24 hours in darkness, and phototoxicity was determined using MTT. Briefly, 10 μL of 5 mg/mL MTT solution was added to each cell culture well and incubated for 4 hours. DMSO (100 μL) was then added, cultures were shaken for 10 seconds, and the absorbance at 570 nm was measured using an ELISA reader (Spectra Max 340/Molecular Devices). Each experimental group consisted of independent triplicate. Data are presented as the mean ± SD values.

Clonogenic assay

For cell survival assays, 500 cells of each cell line were seeded into 6-well plates. The following day, cells were incubated with Ce6 or PS-pNP for 6 hours and then exposed to 6 J/cm^2 of light, as described above. After irradiation, cells were washed and incubated in complete medium until further analysis. Cells treated with Ce6 or PS-pNP but not exposed to light were used as a control, as described above. Ten days postirradiation, cells were stained with 0.5% crystal violet suspended in 20% methanol, and colonies containing at least 100 cells were counted. All experiments were carried out in triplicate, and four culture dishes were used per experiment. The total number of macroscopic cell colonies was counted and calculated as colonies per gram of wet tumor tissue.

Flow cytometry analysis of intracellular Ce6 and PS-pNP levels

AsPC-1, MIA PaCa-2, and MIA PaCa-2/ABCG2 cells were plated in 60-mm^2 culture dishes and grown to 80% confluency at 37°C in the presence of 5% CO_2. The culture medium (DMEM or RPMI1640) was then removed, and 980 μL of fresh medium mixed with 20 μL of Ce6 or PS-pNP solution (5 μmol/L final concentration) was added to the cells. Cells were incubated at 37°C in 5% CO_2 for 6 hours and washed with PBS. Cells were then fixed and incubated overnight with an FITC-conjugated ABCG2-specific antibody at 4°C (Santa Cruz Biotechnology: SC-58222). FITC isotype antibody and unstained cells were used as controls. Treated cells were washed twice in 1 mL of PBS and analyzed by FACS using a FACSCalibur flow cytometer (BD Biosciences FACScan) and quantified with CellQuest software (BD Biosciences).

Immunocytochemical analysis of ABCG2 expression

AsPC-1, MIA PaCa-2, and MIA PaCa-2/ABCG2 cells were seeded in 60-mm^2 culture dishes and grown to 80% confluency at 37°C in the presence of 5% CO_2. The culture medium (DMEM or RPMI1640) was then removed, and 980 μL of fresh medium mixed with 20 μL of Ce6 or PS-pNP solution (5 μM final concentration) was added to the cells. Cells were incubated at 37°C in 5% CO_2 for 6 hours and washed with PBS. Cells were fixed by treating with a mixture of methanol and acetone (1:1) and washed three times with PBS. An ABCG2-specific primary antibody (Santa Cruz Biotechnology) was then added (1:200 dilution), and cells were incubated overnight at 4°C. The following day, cells were washed and incubated with an Alexa Fluor 488–conjugated secondary antibody (1:1,000 dilution; Molecular Probes) for 60 minutes at room temperature. Nuclei were then stained with mounting medium containing 6-diamidino-2-phenylindole (DAPI, Vector Laboratories), and slides were viewed by fluorescence microscopy.

Production of singlet oxygen by Ce6 and PS-pNP

Dose-resolved singlet oxygen ($^1O_2$) measurements were performed by direct detection of the near-infrared luminescence emission of oxygen at 1,270 nm, corresponding to a singlet–triplet transition state. The samples were excited by exposure to 670 nm μJ pulses (5-μs duration) generated by a fiber-coupled diode laser operating with a 10-kHz repetition rate. The singlet oxygen luminescence was detected using a PMT detector (model H10330-45, Hamamatsu) with high sensitivity in the near-infrared region. Three bandpass filters (1,220, 1,270, and 1,320 nm) were placed sequentially in front of the photodetector to sample the luminescence spectrum.

Antitumor effect after PDT in xenograft mouse models

To evaluate the efficacy of PDT using Ce6 or PS-pNP *in vivo*, AsPC-1 tumor cells were implanted either in the subcutaneous layer on the back or orthotopically to the pancreas of BALB/c nude mice (6 weeks of age). Subcutaneous tumors were established by inoculating AsPC-1 cells (1×10^7 cells/100 μL) into the mice. When tumor growth reached 150 to 250 mm^3 in volume, 5 mice per group were treated with intravenous injections of 10 mg/kg of Ce6 or PS-pNP. Injection of PBS was used as control. At 6 hours postinjection, mice were anesthetized by intraperitoneal injection of 50 mg/kg Zoletil 50 (Virbac), and the tumors were irradiated with a 670 ± 10 nm laser (Kuk-Je A & SL Co.). The total impact energy of the exposure was 100 J/cm^2 (800 mW, 2 minutes 30 seconds). For establishment of orthotopic pancreatic tumor model, ASPC-1 cells (1×10^6 in 50 μL of Matrigel-containing media) were injected into the pancreas using a 301/2-gauge needle. Three hours prior to laser irradiation, Ce6 (2.5 and 5 mg/kg) or PS-pNP (2.5 and 5 mg/kg) were injected via tail vein. Interstitial PDT (670 nm laser, 100 mW/cm^2, and 50 J/cm^2) was performed on the exteriorized pancreas of the anesthetized mice. After implementation of tumor cells, these mice were then housed under optimal conditions, and the tumor volumes were measured every 2 days using calipers. Tumor volume was estimated using the following equation: $V\ (\text{mm}^3) = (L \times W^2) \times 0.524$, where L = length (the longest dimension) and W = width (perpendicular to the long axis). All procedures of animal research were provided in accordance with the Laboratory Animals Welfare Act, the Guide for the Care and Use of Laboratory Animals. This animal care and use protocol was reviewed and approved by the IACUC in College of Medicine, The Catholic University of Korea (Seoul, Korea; CUMC-2014-0174-01).

Results

Characterization of the Ce6 and PS-pNP

The structures of chlorin e6 and mPEG-bPEI-Ce6 are shown in Supplementary Fig. S1A and S1B, respectively. We first examined the emission wavelengths of the two molecules using UV-Vis spectrophotometer and then measured the size and zeta potential of PS-pNP. The emission wavelength of Ce6 and PS-pNP was 660 and 670 nm, respectively (Supplementary Fig. S2A). In addition, PS-pNP self-assembled nanoparticle was approximately 40 nm in size and had a zeta potential of 35 mV (Supplementary Fig. S2B). PS-PNP was synthesized by chemical coupling of Ce6, a hydrophobic sensitizer to mPEG (Mn = 5 kDa) conjugated to bPEI (Mn = 1.8 kDa). ^{1}H NMR (Supplementary Fig. S2C) and UV-Vis spectrophotometry showed that each bPEI polymer contained three chains of mPEG and one molecule of Ce6; hence, the molecules were designated asmPEG$_3$-bPEI$_1$-Ce6$_1$ (PS-pNP, Mn = 17.4 kDa; Supplementary Fig. S2D).

Expression of ABCG2 in pancreatic cancer cell lines

As mentioned above, ABCG2 plays a major role in inducing drug resistance and determining the efficacy of PDT. To show that ABCG2 is directly related with PDT efficacy, we established MIA PaCa-2 that stably overexpress ABCG2 using retrovirus. The expression of ABCG2 in human pancreatic cancer cell lines was assayed by qPCR, Western blotting, and immunofluorescence staining analyses. As depicted in Fig. 1A, the MIA PaCa-2 cells exhibited lower levels of *ABCG2* gene expression than the AsPC-1 cells. The immunoblot and immunocytochemistry analyses were consistent with this result, as ABCG2 protein was detected at lower levels in the MIA PaCa-2 cell extracts than in those of the AsPC-1 cells (Fig. 1B and C). Finally, the newly generated MIA PaCa-2/ABCG2 cells exhibited significantly higher levels of ABCG2 expression, at both the mRNA and protein levels, than the parental cell line (Fig. 1).

Effects of ABCG2 expression on photosensitizer uptake in pancreatic cancer cell lines

The intracellular levels of the photosensitizers were measured using a fluorometer and FACS analyses. While the fluorometer studies failed to detect a significant difference in the intracellular levels of PS-pNP and Ce6 in MIA PaCa-2 cells after 48 hours, PS-pNP levels were approximately 2-fold higher than the Ce6 levels in both the MIA PaCa-2/ABCG2 and AsPC-1 cell lines at this time point (Fig. 2A). These findings were supported by the results of the FACS analysis (Fig. 2B). The fluorescence peak corresponding to Ce6 was shifted farther to the right in the MIA PaCa-2 sample than in the MIA PaCa-2/ABCG2 samples; however, this shift was not observed with PS-pNP–treated group. FACS and immunocytochemistry analyses also confirmed that the levels of intracellular PS-pNP were higher than the levels of Ce6 in the MIA PaCa-2/ABCG2 cell line (Fig. 3A and B). These data indicate that high levels of ABCG2 expression resulted in a decrease in the intracellular levels of the Ce6 photosensitizer. Furthermore, they demonstrate that these levels could be increased by PS-pNP. We also confirmed the importance of ABCG2 transport function in the intracellular levels of photosensitizers by using its inhibitor, KO143. As shown in Fig. 3B,

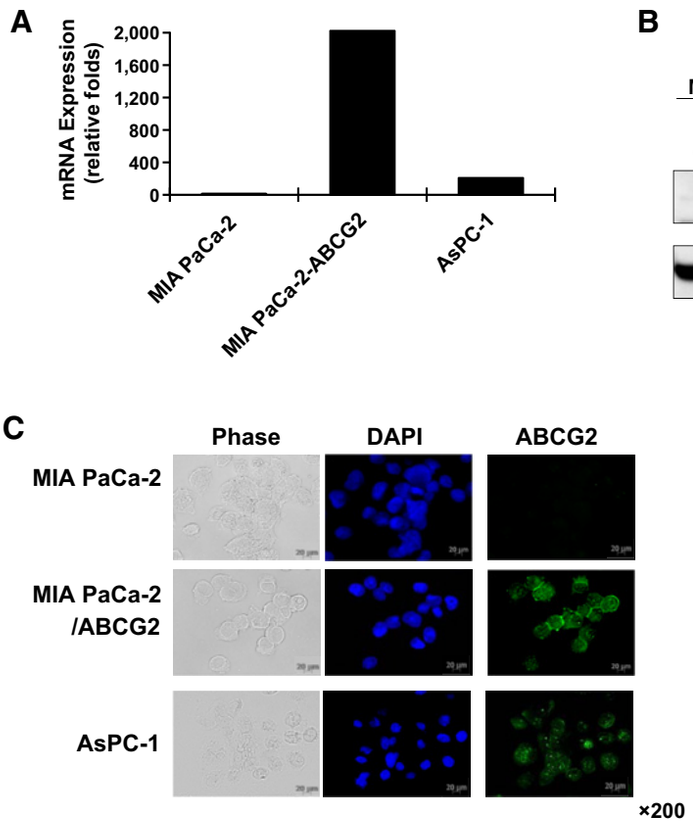

Figure 1.
ABCG2 expression in the pancreatic cancer cells. **A,** qPCR Analysis was used to measure *ABCG2* expression levels in pancreatic cancer cell lines. **B,** Western blot analysis of ABCG2 protein expression in pancreatic cancer cells. MIA PaCa-2/ABCG2 and AsPC-1 cells expressed ABCG2 at variable levels, whereas MIA PaCa-2 cells lacked ABCG2 expression. Approximately 25 μg of protein was used in each lane. The visibility of the actin band was poor at this exposure but was more apparent at longer exposures. **C,** Fluorescence microscopy confirmed the immunocytochemistry of intracellular ABCG2 localization. Methanol/acetone–fixed pancreatic cancer cells were stained using a monoclonal ABCG2-specific antibody and an Alexa 488–labeled secondary antibody. (scale bar, 20 μm)

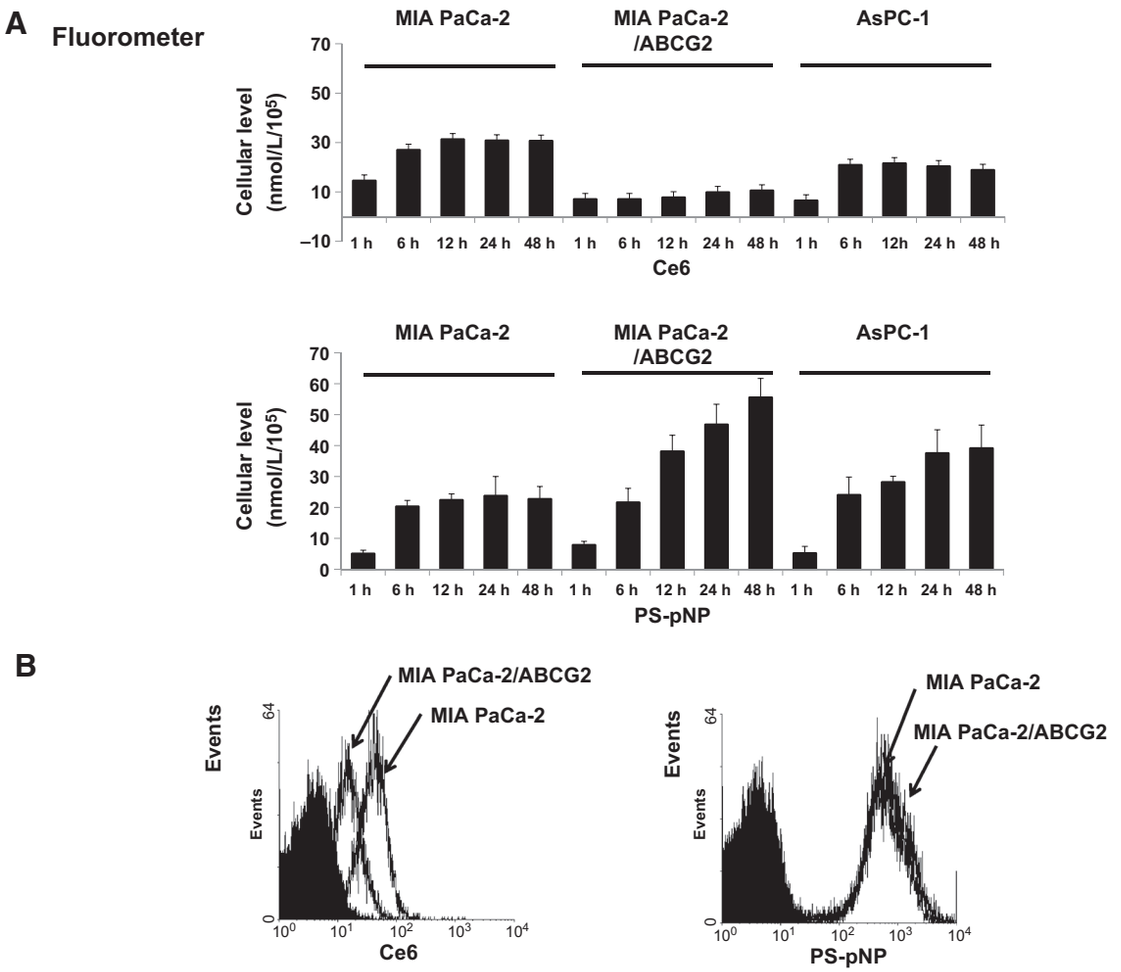

Figure 2.

Photosensitizers in pancreatic cancer cells. **A,** Activation of photosensitizers in pancreatic cancer cell lines at specific time points after PDT treatment. Cells were incubated with 5 μmol/L of Ce6 or PS-pNP, and intracellular photosensitizer concentrations were measured between 3 and 48 hours using a fluorometer. **B,** Histogram analysis of Ce6 and PS-pNP in MIA PaCa-2 and MIA PaCa-2/ABCG2 cells.

KO143 treatment increased cellular level of Ce6, which was not observed in PS-pNP–treated group.

The effects of PDT, using Ce6 or PS-pNP, on viability and survival of pancreatic cancer cells

The viability of pancreatic cancer cell lines was assessed after PDT using either Ce6 or PS-pNP. Although the MIA PaCa-2/ABCG2 cells survived at a significantly higher rate than the MIA PaCa-2 parental cell line after PDT using Ce6 (Fig. 4A), this difference was absent in the samples treated with PDT using PS-pNP (Fig. 4B). To confirm whether the blockage of ABCG2 could increase the effect of PDT, we tested the cell survival rate after treatment of KO143. Combined treatment of Ce6 with KO143 enhanced the sensitivity of PDT (Fig. 4A). Contrastingly, KO143 does not affect cell survival in the PS-pNP–treated cells (Fig. 4B). Dark toxicity was not significant for tested compounds (Fig. 4C). We therefore considered that the survival rate of the MIA PaCa-2/ABCG2 cells decreased as the PS-pNP concentration increased (Fig. 4D).

Singlet oxygen production in Ce6 and PS-pNP–treated pancreatic cancer cell lines

In photodynamic therapy using photosensitizers, production of singlet oxygen is a basic and important mechanism for its cytotoxicity effect. To assess the degree to which PDT treatments affected the pancreatic cancer cell lines, we measured intracellular levels of $^1O_2$. As presented in Fig. 5, there was no significant difference in $^1O_2$ production in the MIA PaCa-2 cells after PDT using either Ce6 or PS-pNP. In contrast, $^1O_2$ levels were lower post-PDT in the MIA PaCa-2/ABCG2 and AsPC-1 cell lines treated with Ce6 than in those treated with PS-pNP. These findings were consistent with the intracellular levels of each photosensitizer, indicating that the PDT-induced cytotoxicity is positively correlated with the intracellular concentration of Ce6.

Antitumor effects of PDT, using Ce6 or PS-pNP, in tumor-xenografted mouse models

To examine the *in vivo* effects of PDT after treatment with Ce6 or PS-pNP, heterotopic or orthotopic tumor-xenografted mouse

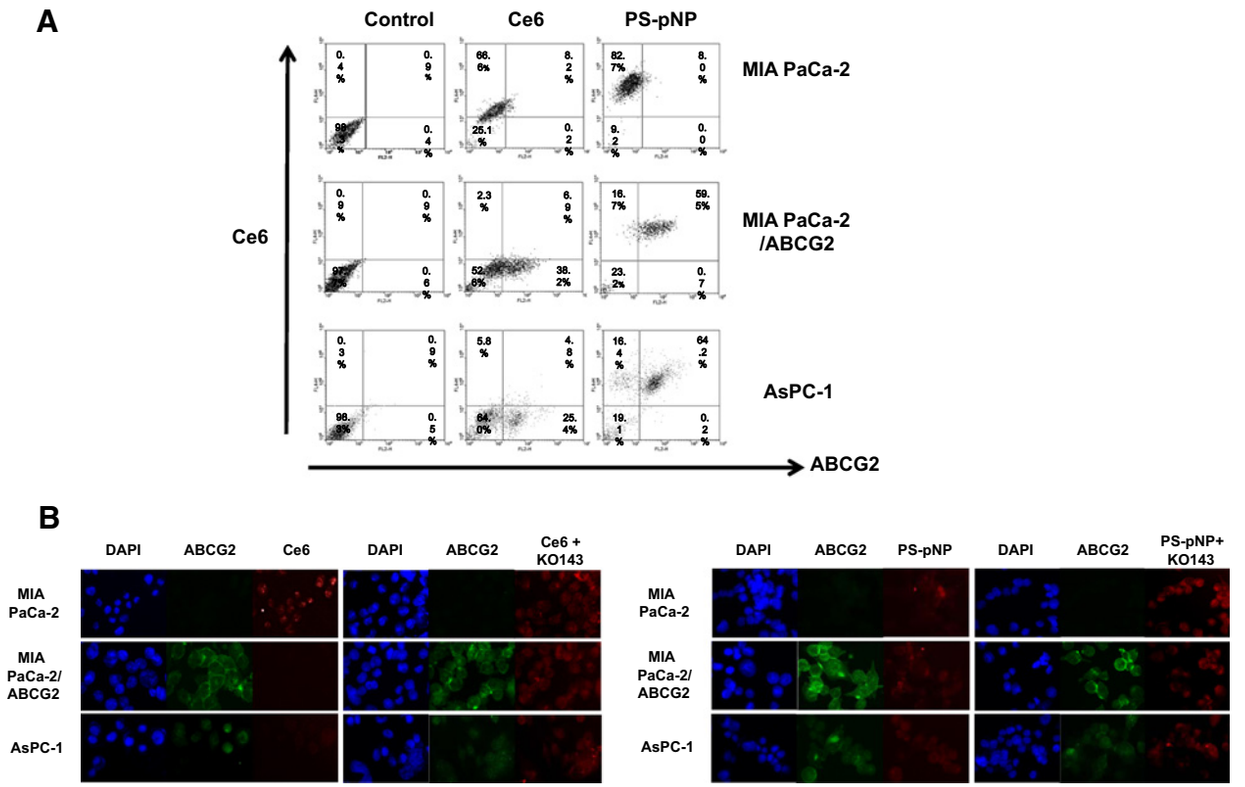

Figure 3.

ABCG2 expression and photosensitizer function in pancreatic cell lines. **A,** Membrane expression of ABCG2 in pancreatic cell lines was measured using flow cytometry. Cells were incubated with 5 μmol/L Ce6 or PS-pNP for 6 hours in the presence or absence of 1 μmol/L Ko-143. ABCG2 expression and photosensitizer levels are indicated for each area. **B,** Fluorescence microscopy of pancreatic cell lines using a FITC-labeled, ABCG2-specific antibody. Nuclei were treated with DAPI stain (red, photosensitizer; green, ABCG2 labeling; and blue, DAPI). MIA PaCa-2/ABCG2, ABCG2-overexpressing MIA PaCa-2 cells; KO-143, ABCG2 inhibitor.

models were utilized (Fig. 6). The data presented in Fig. 6A indicate that only those tumors treated by PDT using PS-pNP were reduced in volume, compared with the tumors of mice in the control group. These results suggest that even a single application of PS-pNP-PDT can effectively inhibit the progression of a solid tumor *in vivo*. We further validated these results in an orthotopic pancreatic cancer and xenograft mouse model. The data presented in Fig. 6B indicate that only those tumors treated by PDT using PS-pNP were reduced in volume, compared with the tumors of mice in the control group. These results suggest that even a single application of PS-pNP-PDT can effectively inhibit the progression of a solid tumor *in vivo*.

Discussion

This study showed that the expression levels of the ABCG2 transporter protein directly correlated to the intracellular accumulation of the Ce6 in pancreatic tumor cells. Both the ABCG2 overexpression–induced MIA PaCa-2 cells as well as naturally high ABCG2-expressing AsPC-1 cells exhibited reduced intracellular levels of Ce6 than the MIA PaCa-2 cells. This decrease in Ce6 concentration was associated with reduced efficacy of PDT-induced cytotoxicity. However, even in pancreatic tumor cells expressing high levels of ABCG2, the use of cationic PS-pNP enhanced the PDT-induced cytotoxicity by increasing the intracellular levels of the photosensitizer, which was demonstrated not only *in vitro* but also *in vivo*. These results indicate that cationic PS-pNP inhibits the ability of the ABCG2 transporter to efflux this compound.

Epithelial cells in the gastrointestinal tract express ABCG2 protein (18), whose function has been regarded as physiologic protection against environmental insults, such as dietary xenobiotics. ABCG2 is also a potential marker of cancer stem cells along with an important mechanism in multidrug resistance (19). In gastrointestinal side-population cells, ABCG2 is overexpressed (20). Because these proteins are overexpressed in many cancers, the function of ABCG2 is regarded as a protection mechanism from xenobiotic toxins in cancer cells (21).

Breast and lung cancer cells expressing increased levels of ABCG2 exhibited decreased levels of the intracellular photosensitizer and were less sensitive to PDT *in vitro* (13, 22, 23). Pancreatic cancer cells present higher levels of ABCG2 than normal parenchymal cells (24). ABCG2 expression is also regarded as one of the key determination factors in the production of side populations that possess stem cell characteristics in many tumors (25, 26). Several studies have shown that ABCG2 blocks the intracellular accumulation of chlorins and molecules with heme structures in various tissues (27, 28). It is believed that this ability also confers resistance to certain cytotoxic drugs, including Ce6 and other photosensitizers (29–31).

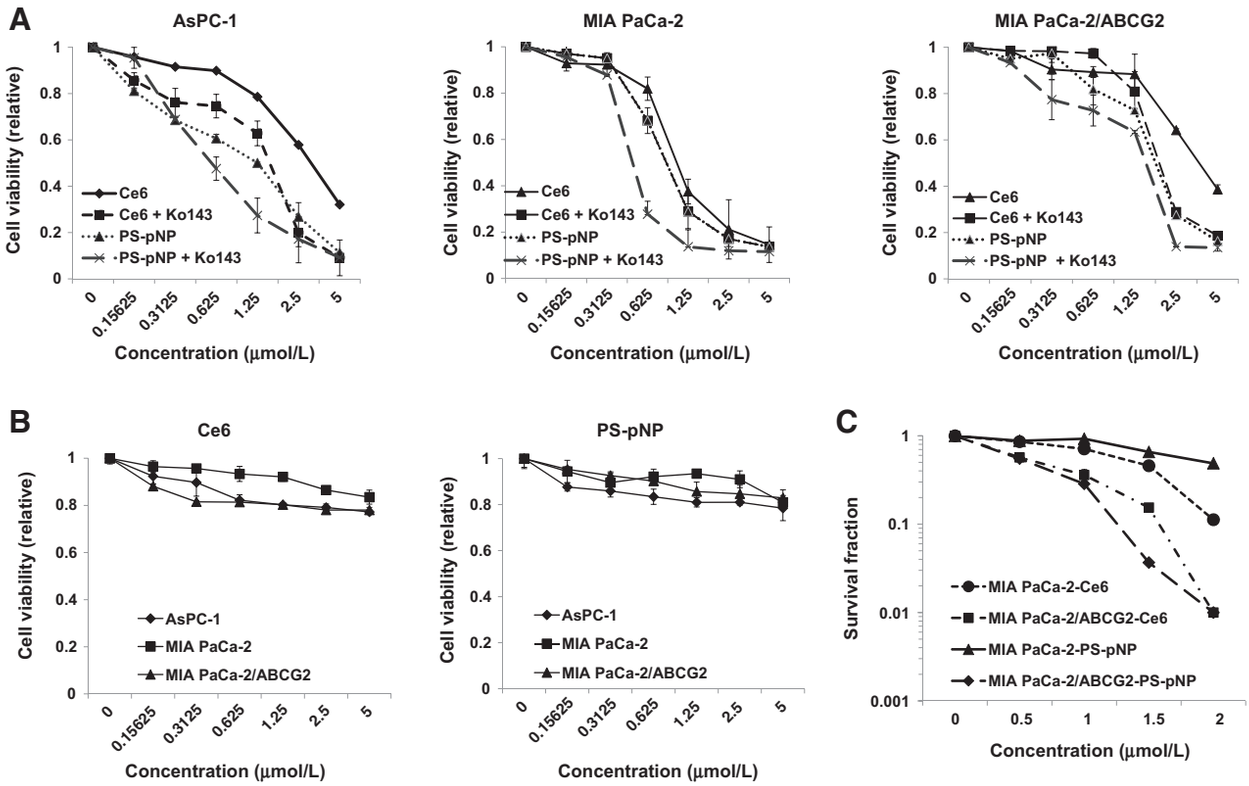

Figure 4.

Phototoxicity of photosensitizers in pancreatic cancer cell lines. **A,** Phototoxicity of Ce6 and PS-pNP in MIA PaCa-2, MIA PaCa-2/ABCG2, and AsPC-1 cells. These cells were irradiated to 670 nm light (6 J/cm^2) after 6-hour incubation with indicated concentration of Ce6 or PS-pNP in the presence or absence of 1 μmol/L KO143. At 24 hours after PDT, the MTT assay was performed. **B,** Dark toxicity of Ce6 and PS-pNP. **C,** MIA PaCa-2/ABCG2, MIA PaCa-2 cells showed cell survival after PDT using photosensitizer.

Gemcitabine is the most commonly used chemotherapeutic agent for pancreatic cancer. The lack of significant clinical response to chemotherapy is explained not only by impaired drug delivery to target due to the highly desmoplastic nature and poor vascularization of pancreatic cancer but also by the drug resistance of pancreatic cancer cells due to drug efflux pumps (32). P-glycoprotein, the best characterized ABC transporter, and others such as ABCC1, ABCC3, ABCC4, and ABCC5 are implicated in drug resistance in pancreatic tumors (32–34) and conferred resistance to pancreatic cell lines against common chemotherapeutic drugs, including gemcitabine and 5-fluorouracil (35, 36).

ABCG2 can also transport a large variety of hydrophobic drugs or drug conjugates, and photosensitizers are the cases. In this study, we have shown that PDT using cationic PS-pNP could overcome the influence of ABCG2. The PS-pNP comprises of PEG, PEI, and Ce6. Intracellular uptake of a photosensitizer is regulated by the ABC transporter superfamily member ABCG2. ABCG2-null mice are more sensitive to skin phototoxicity, which is caused by accumulation of pheophorbide, a chlorophyll degradation product found in a lot of green plant foods (37). This shows the role of ABCG2 in preventing phototoxicity. A separate study demonstrated that overexpression of ABCG2 induced resistance to PDT by blocking the accumulation of the photosensitizer in tumor cells (38). The results of our current study are consistent with these previous findings and provide the first analysis of the relevance of ABCG2 expression to the treatment of pancreatic cancer. We have shown that tumor cell lines with lower levels of ABCG2 expression were more sensitive to PDT than those with higher levels of ABCG2 expression. Together, these studies verify that ABCG2 expression plays a major role in the efficacy of PDT. Furthermore, due to the clinical relevance of ABCG2 in pancreatic tumors, our results suggest that controlling the expression of ABCG2 may be a critical issue for the treatment of this disease.

Several studies have shown that PDT induces cell death in pancreatic cancer cells (39, 40). Small-scale clinical trials have evaluated the efficacy of PDT in patients with inoperable pancreatic cancers and found that the treatment resulted in selective necrotizing of tumor tissues, and prolonged survival of patients receiving the therapy (41, 42). However, these reports also showed considerable variation in the necrosis volume of pancreatic tumors after PDT, suggesting the presence of heterogeneous characteristics in pancreatic tumors, including putative differences in the expression of ABCG2.

The enhanced efficacy can be explained with two mechanisms. First, pegylation attaches PEG covalently to a photosensitizer, which increases the photosensitizer size in solution and also provides water solubility. Pegylation of Ce6 increases the molecular size of photosensitizer, which can decrease the efflux function of ABCG2, increasing the intracellular Ce6 concentration, as

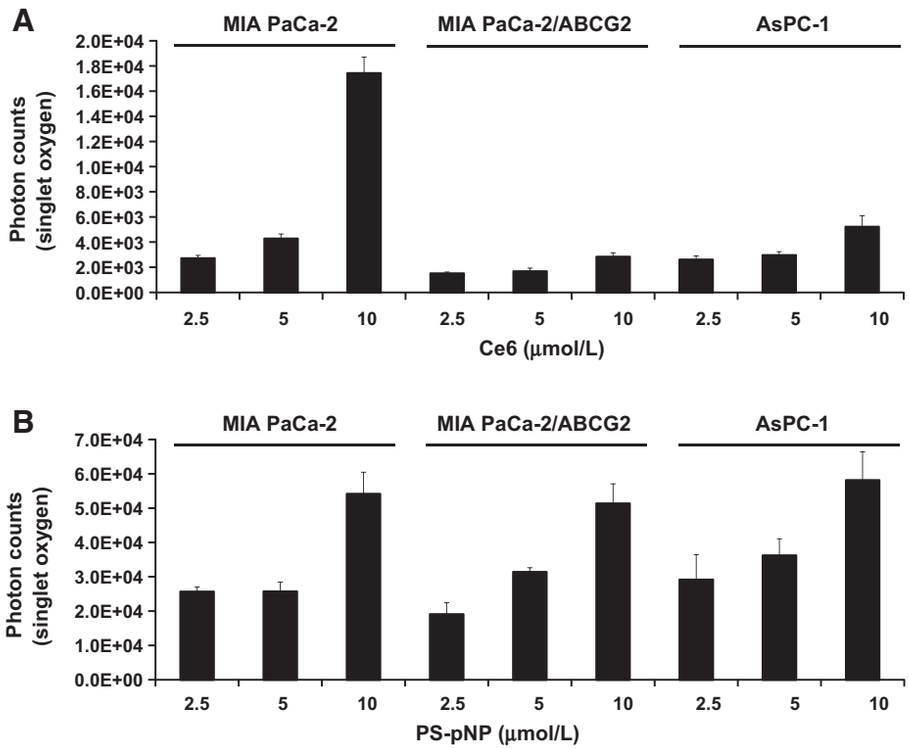

Figure 5.
Measurement of singlet oxygen production. Singlet oxygen kinetics of Ce6 (**A**) and PS-pNP (**B**) upon irradiation at 670 nm μJ pulses (5 μs duration). Pulses were generated using a fiber-coupled diode laser operating with a 10-kHz repetition rate.

shown in our results. Prior reports employed similar conjugates with a goal of high efficacy of PDT, in which photosensitizers were pegylated alone or with poly-L-lysine (43, 44), or protease-sensitive peptides (45, 46). Second, PEI, another component of the PS-pNP, may participate in the enhanced PDT efficacy. The advantage of our photosensitizer is the simple synthesis using non-polylysine PEI and is relatively less toxic by using lower molecular weight compared with polylysine. PEI is not only able to work as a hydrophilic backbone but can also provide a positive charge for the PS-pNP complex with a negative-charged polysaccharide quencher. Another study used PEI conjugate to Ce6 as an antimicrobial photosensitizer (47). However, if only PEI is used for conjugation, it will be aggregated with serum albumin by electrostatic interaction, resulting in macrophage uptake without reaching to target tissues. Generally, the modification of the nanoparticles with PEG results in reduced drug internalization. However, we used PEI having positive charge as well as PEG having negative charge. The average zeta potential is the surface

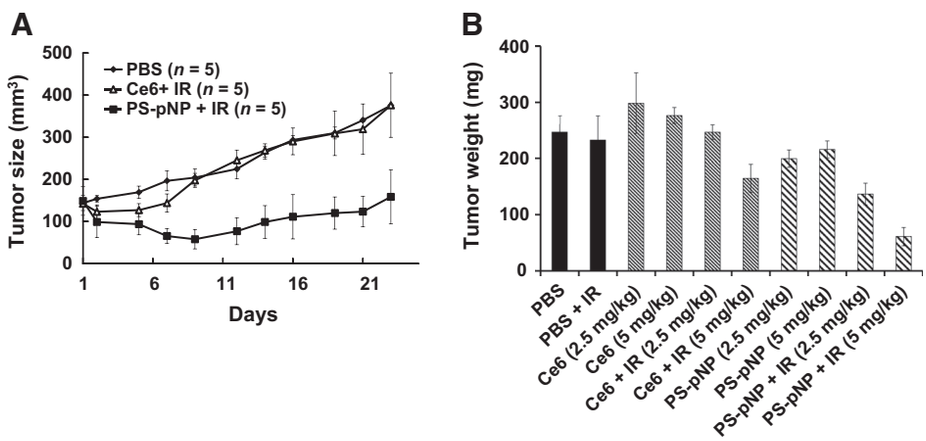

Figure 6.
Antitumor effects of PDT after treatment with Ce6 or PS-pNP in BALB/c nude mice bearing implanted AsPC-1 tumors. **A,** Experiments from subcutaneously implanted pancreatic tumor model. Five mice per group were injected intravenously with Ce6 (10 mg/kg), PS-pNP (10 mg/kg), or a PBS control. Beginning at 6 hours postinjection, tumors were irradiated with a 670 ± 10 nm laser (total impact energy of 100 J/cm^2). The mice were then housed under optimal conditions, and the tumor volumes were measured every 2 days using calipers. **B,** Experiments in orthotopically implanted pancreatic tumor model. Ce6 (2.5 or 5 mg/kg), cationic PS-pNP (2.5 or 5 mg/kg), or PBS were injected to 8 mice per group via tail nein. Beginning at 3 hours postinjection, tumors were irradiated with a 670 ± 10 nm laser (total impact energy of 50 J/cm^2). Interstitial PDT was performed on the exteriorized pancreas of the anesthetized mice with orthotopic tumors. IR, irradiation.

charge because it was synthesized using these two. Zeta potential of our nanoparticle was 35 mVs, which means the positive charge of PEI dominates the negative charge of PEG. Therefore, the enhanced drug internalization could be produced by the positive charge of PEI. This could decrease the possible charge–charge interactions between the drug-exporting protein and Ce6. To specify the exact mechanism, the compounds of Ce6, PEG-ce6, PEI-Ce6, and PEG-PEI-ce6 should be compared. This is our limitation of the current study.

Figure 2 shows the degree of cellular uptake by photosensitizers. This result shows that all AsPC-1, MIA PaCa-2, and MIA PaCa-2/ABCG2 cells in Ce6 are subjected to drug equilibration and saturation, which was observed only in AsPC-1 and MIA PaCa-2 cells by use of PS-pNP. In the MIA PaCa-2/ABCG2 cells, continuous uptake of PS-pNP was observed for 48 hours. This phenomenon is mainly observed in damaged or dead cells. Therefore, we designed *in vivo* experiments further to understand the continuous uptake of PS-pNP in *in vitro* experiments and to carry out the conditions more optimally. For this reason, animal experiments were performed using AsPC-1 cells without using MIA PaCa-2/ABCG2 cells.

The effects of ABCG2 expression on the efficacy of PDT have been evaluated in several other cancer cell types, including breast, lung, and oral cancer cells (11, 23, 48), showing that ABCG2 also conferred resistance to photofrin-based photosensitizers. These results suggest that controlling ABCG2 expression is necessary to attain the intracellular concentrations of a photosensitizer necessary for efficient PDT, and many studies have shown consistent results (11, 13, 22, 23). Thus, evaluating the expression levels of ABCG2 can be a reliable method for predicting the efficacy of photofrin-based PDT and may thereby allow for individualization of this treatment modality (12, 22).

In conclusion, high levels of ABCG2 expression inhibit PDT-induced cytotoxicity in pancreatic cancer cells by reducing intracellular concentrations of chlorin-based photosensitizers. Complexes of Ce6, PEG, and PEI can be an effective method for enhancing PDT efficacy by maximizing intracellular concentrations of the photosensitizer, even in ABCG2-overexpressing pancreatic cancer cells.

Disclosure of Potential Conflicts of Interest

No potential conflicts of interest were disclosed.

Authors' Contributions

Conception and design: Y.J. Roh, I.-W. Kim, K. Na, J.M. Park, M.-G. Choi
Development of methodology: Y.J. Roh, I.-W. Kim, K. Na, J.M. Park, M.-G. Choi
Acquisition of data (provided animals, acquired and managed patients, provided facilities, etc.): Y.J. Roh, I.-W. Kim
Analysis and interpretation of data (e.g., statistical analysis, biostatistics, computational analysis): Y.J. Roh, I.-W. Kim, J.M. Park, M.-G. Choi
Writing, review, and/or revision of the manuscript: Y.J. Roh, K. Na, J.M. Park, M.-G. Choi
Administrative, technical, or material support (i.e., reporting or organizing data, constructing databases): Y.J. Roh, J.H. Kim, I.-W. Kim, J.M. Park
Study supervision: J.M. Park, M.-G. Choi

Acknowledgments

We thank Professor Tayyaba Hasan and Dr. Seonghoon Kim, Wellman Center for Photomedicine, Massachusetts General Hospital, Harvard Medical School, for study supervision and technical support.

Grant Support

This study was supported by a grants (NRF-2011-0031644) from the Global Research and Development Center through the National Research Foundation of Korea funded by the Ministry of Science, ICT and Future Planning (to M.-G. Choi).

The costs of publication of this article were defrayed in part by the payment of page charges. This article must therefore be hereby marked *advertisement* in accordance with 18 U.S.C. Section 1734 solely to indicate this fact.

Received September 27, 2016; revised February 1, 2017; accepted April 5, 2017; published OnlineFirst April 17, 2017.

References

1. Hawes RH, Xiong Q, Waxman I, Chang KJ, Evans DB, Abbruzzese JL. A multispecialty approach to the diagnosis and management of pancreatic cancer. Am J Gastroenterol 2000;95:17–31.
2. Li D, Xie K, Wolff R, Abbruzzese JL. Pancreatic cancer. Lancet 2004; 363:1049–57.
3. Konan YN, Gurny R, Allemann E. State of the art in the delivery of photosensitizers for photodynamic therapy. J Photochem Photobiol B 2002;66:89–106.
4. Lovell JF, Liu TW, Chen J, Zheng G. Activatable photosensitizers for imaging and therapy. Chem Rev 2010;110:2839–57.
5. Chatlani P, Nuutinen P, Toda N, Barr H, MacRobert A, Bedwell J, et al. Selective necrosis in hamster pancreatic tumours using photodynamic therapy with phthalocyanine photosensitization. Br J Surg 1992;79: 786–90.
6. Regula J, Ravi B, Bedwell J, MacRobert A, Bown S. Photodynamic therapy using 5-aminolaevulinic acid for experimental pancreatic cancer–prolonged animal survival. Br J Cancer 1994;70:248.
7. Chan HH, Nishioka NS, Mino M, Lauwers GY, Puricelli WP, Collier KN, et al. EUS-guided photodynamic therapy of the pancreas: a pilot study. Gastrointest Endosc 2004;59:95–9.
8. Bown S, Rogowska A, Whitelaw D, Lees W, Lovat L, Ripley P, et al. Photodynamic therapy for cancer of the pancreas. Gut 2002;50:549–57.
9. Robey RW, To KK, Polgar O, Dohse M, Fetsch P, Dean M, et al. ABCG2: a perspective. Adv Drug Deliv Rev 2009;61:3–13.
10. Ishikawa T, Nakagawa H. Human ABC transporter ABCG2 in cancer chemotherapy and pharmacogenomics. J Exp Ther Oncol 2009;8:5–24.
11. Liu W, Baer MR, Bowman MJ, Pera P, Zheng X, Morgan J, et al. The tyrosine kinase inhibitor imatinib mesylate enhances the efficacy of photodynamic therapy by inhibiting ABCG2. Clin Cancer Res 2007;13:2463–70.
12. Hagiya Y, Endo Y, Yonemura Y, Takahashi K, Ishizuka M, Abe F, et al. Pivotal roles of peptide transporter PEPT1 and ATP-binding cassette (ABC) transporter ABCG2 in 5-aminolevulinic acid (ALA)-based photocytotoxicity of gastric cancer cells *in vitro*. Photodiagnosis Photodyn Ther 2012;9:204–14.
13. Morgan J, Jackson JD, Zheng X, Pandey SK, Pandey RK. Substrate affinity of photosensitizers derived from chlorophyll-a: the ABCG2 transporter affects the phototoxic response of side population stem cell-like cancer cells to photodynamic therapy. Mol Pharm 2010;7:1789–804.
14. Wang F, Xue X, Wei J, An Y, Yao J, Cai H, et al. hsa-miR-520h downregulates ABCG2 in pancreatic cancer cells to inhibit migration, invasion, and side populations. Br J Cancer 2010;103:567–74.
15. Yuan Y, Yang Z, Miao X, Li D, Liu Z, Zou Q. The clinical significance of FRAT1 and ABCG2 expression in pancreatic ductal adenocarcinoma. Tumour Biol 2015;36:9961–8.
16. Park W, Park SJ, Na K. The controlled photoactivity of nanoparticles derived from ionic interactions between a water soluble polymeric photosensitizer and polysaccharide quencher. Biomaterials 2011;32: 8261–70.
17. Kim GM, Bae YH, Jo WH. pH-induced micelle formation of poly (histidine-co-phenylalanine)-block-poly (ethylene glycol) in aqueous media. Macromol Biosci 2005;5:1118–24.

18. Gutmann H, Hruz P, Zimmermann C, Beglinger C, Drewe J. Distribution of breast cancer resistance protein (BCRP/ABCG2) mRNA expression along the human GI tract. Biochem Pharmacol 2005;70:695–9.
19. Kitamura H, Okudela K, Yazawa T, Sato H, Shimoyamada H. Cancer stem cell: implications in cancer biology and therapy with special reference to lung cancer. Lung Cancer 2009;66:275–81.
20. Haraguchi N, Utsunomiya T, Inoue H, Tanaka F, Mimori K, Barnard GF, et al. Characterization of a side population of cancer cells from human gastrointestinal system. Stem Cells 2006;24:506–13.
21. Lou H, Dean M. Targeted therapy for cancer stem cells: the patched pathway and ABC transporters. Oncogene 2007;26:1357–60.
22. Tracy EC, Bowman MJ, Pandey RK, Henderson BW, Baumann H. Cell-type selective phototoxicity achieved with chlorophyll-a derived photosensitizers in a co-culture system of primary human tumor and normal lung cells. Photochem Photobiol 2011;87:1405–18.
23. Usuda J, Tsunoda Y, Ichinose S, Ishizumi T, Ohtani K, Maehara S, et al. Breast cancer resistant protein (BCRP) is a molecular determinant of the outcome of photodynamic therapy (PDT) for centrally located early lung cancer. Lung Cancer 2010;67:198–204.
24. Mohelnikova-Duchonova B, Brynychova V, Oliverius M, Honsova E, Kala Z, Muckova K, et al. Differences in transcript levels of ABC transporters between pancreatic adenocarcinoma and nonneoplastic tissues. Pancreas 2013;42:707–16.
25. Zhou S, Schuetz JD, Bunting KD, Colapietro AM, Sampath J, Morris JJ, et al. The ABC transporter Bcrp1/ABCG2 is expressed in a wide variety of stem cells and is a molecular determinant of the side-population phenotype. Nat Med 2001;7:1028–34.
26. Wu C, Wei Q, Utomo V, Nadesan P, Whetstone H, Kandel R, et al. Side population cells isolated from mesenchymal neoplasms have tumor initiating potential. Cancer Res 2007;67:8216–22.
27. Krishnamurthy P, Xie T, Schuetz JD. The role of transporters in cellular heme and porphyrin homeostasis. Pharmacol Ther 2007;114:345–58.
28. Wakabayashi K, Tamura A, Saito H, Onishi Y, Ishikawa T. Human ABC transporter ABCG2 in xenobiotic protection and redox biology. Drug Metab Rev 2006;38:371–91.
29. Han B, Zhang JT. Multidrug resistance in cancer chemotherapy and xenobiotic protection mediated by the half ATP-binding cassette transporter ABCG2. Curr Med Chem Anticancer Agents 2004;4:31–42.
30. Lage H. ABC-transporters: implications on drug resistance from microorganisms to human cancers. Int J Antimicrob Agents 2003;22:188–99.
31. Leslie EM, Deeley RG, Cole SP. Multidrug resistance proteins: role of P-glycoprotein, MRP1, MRP2, and BCRP (ABCG2) in tissue defense. Toxicol Appl Pharmacol 2005;204:216–37.
32. Zhou J, Liu M, Aneja R, Chandra R, Lage H, Joshi HC. Reversal of P-glycoprotein-mediated multidrug resistance in cancer cells by the c-Jun NH2-terminal kinase. Cancer Res 2006;66:445–52.
33. Konig J, Hartel M, Nies AT, Martignoni ME, Guo J, Buchler MW, et al. Expression and localization of human multidrug resistance protein (ABCC) family members in pancreatic carcinoma. Int J Cancer 2005;115:359–67.
34. Kool M, van der Linden M, de Haas M, Scheffer GL, de Vree JM, Smith AJ, et al. MRP3, an organic anion transporter able to transport anti-cancer drugs. Proc Natl Acad Sci U S A 1999;96:6914–9.
35. Hagmann W, Jesnowski R, Lohr JM. Interdependence of gemcitabine treatment, transporter expression, and resistance in human pancreatic carcinoma cells. Neoplasia 2010;12:740–7.
36. Nambaru PK, Hubner T, Kock K, Mews S, Grube M, Payen L, et al. Drug efflux transporter multidrug resistance-associated protein 5 affects sensitivity of pancreatic cancer cell lines to the nucleoside anticancer drug 5-fluorouracil. Drug Metab Dispos 2011;39:132–9.
37. Jonker JW, Buitelaar M, Wagenaar E, Van Der Valk MA, Scheffer GL, Scheper RJ, et al. The breast cancer resistance protein protects against a major chlorophyll-derived dietary phototoxin and protoporphyria. Proc Natl Acad Sci U S A 2002;99:15649–54.
38. Ishikawa T, Nakagawa H, Hagiya Y, Nonoguchi N, Miyatake S, Kuroiwa T. Key role of human ABC transporter ABCG2 in photodynamic therapy and photodynamic diagnosis. Adv Pharmacol Sci 2010;2010:587306.
39. Wang LW, Huang Z, Lin H, Li ZS, Hetzel F, Liu B. Effect of Photofrin-mediated photocytotoxicity on a panel of human pancreatic cancer cells. Photodiagnosis Photodyn Ther 2013;10:244–51.
40. Xie Q, Jia L, Liu YH, Wei CG. Synergetic anticancer effect of combined gemcitabine and photodynamic therapy on pancreatic cancer *in vivo*. World J Gastroenterol 2009;15:737–41.
41. Pereira S. Photodynamic therapy for pancreatic and biliary tract cancer: the United Kingdom experience. J Natl Compr Canc Netw 2012;10:S48–51.
42. Fan BG, Andren-Sandberg A. Photodynamic therapy for pancreatic cancer. Pancreas 2007;34:385–9.
43. Hamblin MR, Miller JL, Rizvi I, Loew HG, Hasan T. Pegylation of charged polymer-photosensitiser conjugates: effects on photodynamic efficacy. Br J Cancer 2003;89:937–43.
44. Hamblin MR, Miller JL, Rizvi I, Ortel B, Maytin EV, Hasan T. Pegylation of a chlorin(e6) polymer conjugate increases tumor targeting of photosensitizer. Cancer Res 2001;61:7155–62.
45. Choi Y, Weissleder R, Tung CH. Selective antitumor effect of novel protease-mediated photodynamic agent. Cancer Res 2006;66:7225–9.
46. Choi Y, Weissleder R, Tung CH. Protease-mediated phototoxicity of a polylysine-chlorin(E6) conjugate. Chem Med Chem 2006;1:698–701.
47. Tegos GP, Anbe M, Yang C, Demidova TN, Satti M, Mroz P, et al. Protease-stable polycationic photosensitizer conjugates between polyethyleneimine and chlorin(e6) for broad-spectrum antimicrobial photoinactivation. Antimicrob Agents Chemother 2006;50:1402–10.
48. Yamamoto M, Fujita H, Katase N, Inoue K, Nagatsuka H, Utsumi K, et al. Improvement of the efficacy of 5-aminolevulinic acid-mediated photodynamic treatment in human oral squamous cell carcinoma HSC-4. Acta Med Okayama 2013;67:153–64.